Transfer induced by core excitation within an extended distorted-wave Born approximation method

M. Gómez-Ramos, A. M. Moro, J. Gómez-Camacho, and I. J. Thompson

Transfer induced by core excitation within an extended DWBA method

M. Gómez-Ramos* and A. M. Moro†

Departamento de FAMN, Facultad de Física, Universidad de Sevilla,Apdo. 1065, E-41080 Sevilla, Spain

J. Gómez-Camacho‡

*Departamento de FAMN, Facultad de Física, Universidad de Sevilla,Apdo. 1065, E-41080 Sevilla, Spain and
Centro Nacional de Aceleradores, Avda. Thomas A. Edison, E-41092, Sevilla, Spain*

I. J. Thompson§

Lawrence Livermore National Laboratory, L-414, Livermore, California 94551, USA
(Dated: June 1, 2015)

Background:: Dynamic core excitation effects have been found to be of importance in breakup reactions and may be of relevance when obtaining spectroscopic information from transfer reactions.

Purpose:: In this paper we extend the distorted-wave Born approximation (DWBA) formalism in order to allow for non-central components in the core-core term appearing in the transition operator, which allows for dynamic core excitation effects. Then we study these effects applying the formalism to different (d,p) reactions.

Methods:: The expression of the non-local kernels required for the evaluation of the DWBA amplitudes has been extended so as to include non-central parts in the core-core interaction. The DWBA scattering amplitude has been then obtained by solving the corresponding inhomogeneous equation, with the new computed kernels, and the usual outgoing boundary conditions. A new DWBA code has been developed for this purpose.

Results:: For $^{10}\text{Be}(d,p)^{11}\text{Be}$, core excitations effects are found to be almost negligible ($< 3\%$). The importance of this effect has been found to depend to a large extent on the excitation energy of the core. This has been confirmed in the $^{30}\text{Ne}(d,p)^{31}\text{Ne}$ case, for which the excitation energy of the first 2^+ state is 0.8 MeV, and the effect of core excitation increases to 10%

Conclusions:: We find dynamic core excitation effects in transfer reactions to have small contributions to cross sections, in general. However, they should not be neglected, since they may modify the spectroscopic information obtained from these reactions and may become of importance in reactions with nuclei with a core with high deformation and low excitation energy.

I. INTRODUCTION

Transfer reactions have for decades been one of the main sources of information on the structure of stable and, more recently, also of exotic nuclei. The angular distribution of the outgoing particles produced in these processes is very sensitive to the transferred orbital angular momentum between the projectile and target, whereas the magnitude depends on the product of the initial and final spectroscopic factors (the normalization of the overlap functions in the initial and final nuclei).

Extraction of accurate structure information from these measurements relies on the comparison of the data (often angular distributions) with calculations using a suitable reaction formalism. Traditionally, the analysis of transfer reactions has been carried out in terms of the distorted-wave Born approximation (DWBA). Corrections and improvements of this method have also been used. For example, when the initial or final nuclei contain collective excited states, multistep processes involving excitations and deexcitations among these states can be

suitably incorporated within the coupled-channels Born approximation (CCBA) method [1]. Moreover, when one the colliding nuclei is weakly bound, such as in the case of (d,p) reactions, coupling effects to breakup channels can also influence the transfer cross sections and hence the inclusion of these couplings become important. This has been done within the CDCC (Continuum-Discretized Coupled Channels) approximation [2–6] or, more simply, within the adiabatic approximation, such as in the adiabatic distorted wave approximation (ADWA) of Johnson and Tandy [7]. More recently, the Alt-Grasberger-Sandhas (AGS) formulation of the Faddeev equations [8, 9] has also been successfully applied to transfer reactions (see [10] for a recent review of these methods).

In a simple picture, a transfer reaction can be modelled in a three-body model, in which a nucleon, or group of nucleons, is transferred from one nucleus to another. For example, a stripping reaction of the form $b(d,p)B$ can be viewed as a process in which the incident deuteron transfers a neutron to the target nucleus b, producing a composite nucleus $B = b + n$ in a given state defined by the relative wavefunction of neutron and core b. However, this naive interpretation of the transfer process, which is the basis of the DWBA approximation, neglects possible effects derived from the excitation of the subsystems. Indeed, it is well known that core excitations can affect the transfer process in several ways. First, the interaction

between the transferred particle and the core b will not be given by a simple spherical potential, but will contain non-central terms that will give rise to core-excited admixtures in the states of the composite nucleus B. The weight of each component can be regarded as a spectroscopic factor. This is a structure effect, not related to the reaction mechanism, and will be referred to as *static* core excitation. In actual calculations, this effect can be included using some particle-core model (particle-rotor, particle-vibrator, Nilsson, etc) or, more commonly, by simply multiplying some single-particle wavefunctions by appropriate spectroscopic amplitudes. This is the usual procedure followed in the DWBA method.

Another core excitation effect that may influence this reaction arises from the initial state interaction of the incoming deuteron with the target b. Before the neutron is transferred, the deuteron may induce excitations on the core b, thus altering the population probability of the different core states. These *dynamic* core excitation effects can be conveniently treated within the CCBA method, and are commonly referred to as *multistep* or *coupled-channels* effects. In presence of these additional couplings, the cross sections for the different final states will no longer be proportional to the corresponding spectroscopic factors.

Finally, another way in which core excitation can affect transfer dynamics is through the interaction of the proton with the core b. In the DWBA and CCBA formalisms, this interaction appears in the so-called *remnant* term of the transition operator, and gives rise to a core-recoil effect. Standard calculations consider only the central part of this core-core interaction. However, the presence of non-central parts (e.g. inelastic couplings) in this interaction will give an additional contribution to the transfer cross section, even in Born approximation. In our previous example, these non-central terms could connect different states of the core b, thus affecting the cross sections leading to these states. We will refer to this mechanism as transfer induced by *prompt* core excitation, to distinguish it from the aforementioned *dynamic* (multistep) and *static* core excitation effects.

This problem of prompt core excitation in transfer reactions has been scarcely studied in the literature. In Ref. [11], the problem was studied within the zero-range DWBA approximation and for (d, p) reactions only. The contribution of transfer induced by prompt core excitation was found to be very small ($\sim 6\%$) in most cases studied but the calculations were done with many approximations (the transfer amplitude was evaluated in zero-range, a closed-shell model was used for the core nucleus, and the bound state wavefunctions were approximated by harmonic-oscillator functions) and so the conclusions must be taken with some caution. In Ref. [12], Kozlowsky and de-Shalit proposed a zero-range core-excitation DWBA model for the (^{3}He,d) case. The transfer was also treated in zero-range and core excitation was modelled within the vibrational model. The angular distribution via core excitation was found to be very simi-

lar to that of ordinary stripping due to a single-particle mechanism but the calculated magnitude underpredicted the experimental data by about one order of magnitude. However, this magnitude was found to depend very critically on the radius of the particle-core potential, which is directly linked to the distance at which the stripping mechanism is assumed to occur.

Recently, the problem has been addressed [13] within the AGS formulation of the Faddeev equations [8, 9]. The method was applied to several (d, p) and (p, d) reactions involving the nuclei ^{11}Be and ^{24}Mg. Dynamic core excitation effects were found to be important, often improving the description of the experimental data. Moreover, these effects could not be reproduced by a simple reduction of the cross section by the corresponding spectroscopic factor. It is worth noting however that these calculations include, in an non-trivial way, effects arising from the different sources of core excitation discussed above. In particular, *dynamic* multistep and prompt core excitation effects will appear entangled in this approach, and so the assessment of their relative importance is not straightforward from the final cross sections.

In view of these results, we believe that it is useful to investigate (and isolate) the phenomenon of prompt core excitation within the much simpler DWBA framework. To avoid the limitations of previous calculations of this kind [11, 12], we aim at performing full-fledged DWBA calculations, including finite-range effects and a more realistic model of the core+valence system. With this premise in mind, in this work we present the theoretical formulation of the problem, and apply this model to the ^{10}Be(d,p)^{11}Be and ^{30}Ne(d,p)^{31}Ne reactions.

We finally note that this work follows a series of previous works aimed at understanding the effect of core excitation in the different reaction channels. In Refs. [14–16], the study was focused on the breakup channels, and for that purpose appropriate extensions of the DWBA and Continuum-Discretized Coupled-Channels method were developed and applied to several physical cases. Dynamic core excitation effects were found be small for the case of the scattering with heavy targets but, on the other hand, sizable effects were found for light targets, typically enhancing the breakup cross sections with respect to the inert core case.

The paper is structured as follows. In section II, we present an extended DWBA formalism including prompt core excitation effects. In Sec. III, the method is applied to the ^{10}Be(p,d)^{11}Be and ^{30}Ne(p,d)^{31}Ne reactions and compared with recent data in the former case. The effect of the excitation energy of the core is also studied using a model with a fictitious ^{11}Be nucleus with reduced core excitation energy. In Sec. IV we summarize the main conclusions of this work.

II. THEORETICAL FORMULATION

Let us consider the transfer reaction $A(a + v) + b \rightarrow a + B(b + v)$ in which a composite projectile A transfers a particle v to the target nucleus b giving rise to the ejectile a and the residual composite nucleus B. This is a many-body scattering problem which, under suitable approximations [10, 17], can be reduced to an effective three-body problem. We will consider that nucleus b has internal degrees of freedom (ξ) which are relevant in the reaction. The effective three-body Hamiltonian describing this problem can be expressed in two different forms, depending on whether one chooses the *prior* or *post* representations, i.e.,

$$H_{\text{prior}} = T_R + H_A(\vec{r}) + U_{ab}(\vec{r_c}, \xi) + V_{vb}(\vec{r}', \xi), \quad (1)$$

$$H_{\text{post}} = T_{R'} + H_B(\xi, \vec{r}') + U_{ab}(\vec{r_c}, \xi) + V_{va}(\vec{r}), \quad (2)$$

where T_R and $T_{R'}$ represent the kinetic energy operators for the projectile–target relative motion before and after the transfer reaction, respectively. H_A and H_B are the internal Hamiltonians of the composite systems formed by the valence particle and the core to which it is bound. The real interactions V_{va} and V_{vb} are the binding potentials for the transferred particle in the initial and final nucleus, respectively. Finally, the potential U_{ab}, complex in general, represents the effective interaction between the two cores. Note that possible excitations of a are not considered explicitly (this is indeed justified for the applications presented in the next section, in which a represents a proton). The relevant coordinates are shown in Fig. 1 and obey the following relations

$$\vec{r} = a\vec{R} + b\vec{R}'; \qquad \vec{r}' = a'\vec{R} + b'\vec{R}'; \quad \vec{r_c} = a_c\vec{R} + b_c\vec{R}'$$

$$\nu_A = m_a/m_A; \qquad \nu_B = m_b/m_B; \qquad \omega = \frac{1}{1 - \nu_A \nu_B}$$

$$a = \nu_B \omega; \qquad b = -\omega$$
$$a' = \omega; \qquad b' = -\nu_A \omega$$
$$a_c = -\omega(1 - \nu_B); \quad b_c = -\omega(1 - \nu_A) \qquad (3)$$

Since b is allowed to be excited during the transfer reaction, its wavefunction as well as the interactions U_{ab} and V_{vb} will depend on ξ. Using the *post* representation, the exact transition amplitude can be expressed as (see, for instance, Refs. [1, 18])

$$T_{\beta\alpha} = \langle \Phi_\beta^{(-)}(\vec{r}', \vec{R}', \xi)| \, U_{ab}(\vec{r_c}, \xi) + V_{va}(\vec{r})$$
$$- U_\beta(R') \, |\Psi_\alpha^{(+)}(\vec{r}, \vec{R}, \xi)\rangle, \qquad (4)$$

where $\Psi_\alpha^{(+)}(\vec{r}, \vec{R}, \xi)$ corresponds to the full three-body wave function of the system and $U_\beta(R')$ is an arbitrary potential, which is usually chosen to reproduce the elastic scattering of the $a + B$ system. The final wave function $\Phi_\beta^{(-)}(\vec{r}', \vec{R}', \xi)$ is an eigenstate of the Hamiltonian $H_f = T_{R'} + H_B + H_a$ and can therefore be expressed in the factorized form:

$$\Phi_\beta^{(-)}(\vec{r}', \vec{R}', \xi) = \chi_\beta^{(-)}(\vec{R}')\psi_B(\vec{r}', \xi)\psi_a, \qquad (5)$$

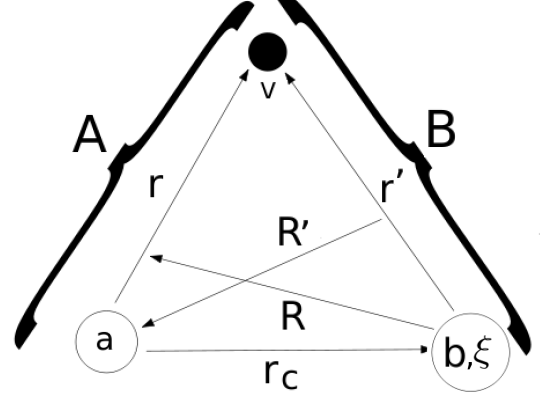FIG. 1. Relevant coordinates involved in the calculation. a and b are the cores to which the valence particle v is bound before and after the transfer reaction.

where ψ_B and ψ_a correspond to the internal wavefunctions of B and a, and $\chi_\beta^{(-)}$ is the distorted wave with incoming boundary conditions obtained by solving Schrödinger equation with the potential U_β.

In the DWBA approximation, the total three-body wave function $\Psi_\alpha^{(+)}$ is approximated by an expression analogous to (5):

$$\Psi_\alpha^{(+)}(\vec{r}, \vec{R}, \xi) \simeq \chi_\alpha^{(+)}(\vec{R})\psi_A(\vec{r})\psi_b(\xi), \qquad (6)$$

where $\psi_{A,b}$ are equivalent to $\psi_{B,a}$ and $\chi_\alpha^{(+)}$ is the distorted wave with outgoing boundary conditions obtained by solving the Schrödinger equation with an optical potential U_α between projectile and target in the incident channel. The DWBA transition amplitude results

$$T_{\beta\alpha}^{DWBA} = \langle \chi_\beta^{(-)}(\vec{R}')\psi_B(\vec{r}', \xi)\psi_a| \, U_{ab}(\vec{r_c}, \xi) + V_{va}(\vec{r})$$
$$- U_\beta(R') \, |\chi_\alpha^{(+)}(\vec{R})\psi_A(\vec{r})\psi_b(\xi)\rangle. \qquad (7)$$

Expanding this expression in partial waves, for a certain total angular momentum J_T, one obtains:

$$T_{\beta\alpha,J_T M_T}^{DWBA} = \frac{(4\pi)^2}{k_\alpha k_\beta} \sum_{\substack{LM,JM_J \\ L'M',J'M'_J}} i^{L-L'} Y_{LM}^*(\hat{\mathbf{k}}_\alpha) Y_{L'M'}(\hat{\mathbf{k}}_\beta) e^{i(\sigma_L + \sigma_{L'})}$$

$$\times \langle LJ_p M M_p | JM_J \rangle \langle L'J'_p M'M'_p | J'M'_J \rangle \langle JJ_t M_J M_t | J_T M_T \rangle \langle J'J'_t M'_J M'_t | J_T M_T \rangle$$

$$\times \int dR\, dR' \chi_{\beta,L',J'}^{(-)}(R') K_{\alpha\beta}(R,R') \chi_{\alpha,L,J}^{(+)}(R), \tag{8}$$

where σ_L are the Coulomb phase shifts, Y_{LM} denote the spherical harmonics and $\chi_{\alpha,L,J}^{(+)}$ and $\chi_{\beta,L',J'}^{(-)}$ are the radial parts of the distorted waves introduced in Eqs. (5) and (6), respectively. J_p and J_t are the spin of the projectile and target respectively in the initial partition, and J'_p and J'_t are the spins of ejectile and residual nucleus in the final partition. J and J' are the result of coupling $L \otimes J_p$ and $L' \otimes J'_p$ respectively. Note that the S-matrix elements, from which the scattering observables can be computed, are related to the T-matrix as $S_{\beta\alpha,J_T M_T} = -2i\pi T_{\beta\alpha,J_T M_T}$. The quantities $K_{\alpha\beta}(R,R')$, usually referred to as non-local *kernels* [1], are defined as

$$K_{\alpha\beta}(R,R') = \int \left[\left[Y_{L'}(\hat{R}') \otimes \psi_a^{J'_p} \right]_{J'} \otimes \psi_B^{J'_t} \right]_{J_T M_T}^* (U_{ab}$$
$$+ V_{va} - U_\beta) \left[\left[Y_L(\hat{R}) \otimes \psi_A^{J_p} \right]_J \otimes \psi_b^{J_t} \right]_{J_T M_T}. \tag{9}$$

They include integration over the angular parts of $\vec{R}$ and $\vec{R}'$ and the internal degrees of freedom of the reacting particles, remaining functions of R and R' only (in modulus). These kernels encompass the transition potential, the internal wave functions of projectile and target in the incoming and outgoing channels and the angular part of the distorted waves in both channels.

The wavefunction of the composite system A $(a+v)$ is expanded as follows

$$\psi_A^{J_p} = \sum_{l,j,s_a} \varphi_{l,j,s_a}(r) \left[[Y_l \otimes \chi_s]_j \otimes \psi_{s_a}^a \right]_{J_p}, \tag{10}$$

where χ_s is the spin function of the valence particle, s_a the intrinsic angular momentum of the core a and l the orbital angular momentum between valence particle and core. Likewise, for the composite nucleus B $(b+v)$,

$$\psi_B^{J'_t} = \sum_{l',j',I'} \varphi'_{l',j',I'}(r') \left[[Y_{l'} \otimes \chi_s]_{j'} \otimes \psi_{I'}^b(\xi) \right]_{J'_t}. \tag{11}$$

The potential U_{ab} depends on $\vec{r}_c$ and ξ. Since it is a scalar, it can be expanded in multipoles, in a way analogous to [19]:

$$U_{ab} = \sum_Q \hat{Q}\, U_{ab}^Q(r_c,\xi) \sum_q C_{Qq}(\hat{r}_c) \mathcal{T}_{Qq}^*(\xi), \tag{12}$$

where $C_{Qq} = \hat{Q} Y_{Qq}/\sqrt{4\pi}$, $\hat{Q} = \sqrt{2Q+1}$ and $\mathcal{T}_{Qq}$ is a function with the same tensorial rank as C_{Qq}. Let us remark that, since the transition potential depends on ξ and is not central in its dependence on $\vec{r}_c$, the transition between different states of the core b, with different angular momenta I,I', is possible during the reaction, in the process which we call prompt core excitation. Inserting the multipole expansion (12) in Eq. (9) it is possible to express the complete kernels $K_{\alpha\beta}(R,R')$ as a sum of terms with different multipoles Q:

$$K_{\alpha\beta}(R,R') = K_{\alpha\beta}^{(Q=0)}(R,R') + K_{\alpha\beta}^{(Q>0)}(R,R') \tag{13}$$

Standard DWBA and CCBA calculations consider only the term with $Q = 0$, and hence they exclude prompt core excitation effects. These effects are induced by the $Q > 0$ terms, which are considered in detail in the following.

Since the angular momentum of the core b is no longer conserved in the reaction and there are non-central components of the potential U_{ab}, it is necessary to recouple the relevant angular momenta in a somewhat more complex way for the kernels with $Q \neq 0$ than in the standard case [20] (see Appendix B).

We now present the resulting form of the kernels and refer to appendix A for more details on their construction. We remark that the particle is transferred from the projectile to the target and the target is a deformed core, with angular momentum I in the incoming channel and I' in the exit channel. This calculation assumes all potentials but U_{ab} to be central, and therefore excludes the spin-orbit terms. Nevertheless, we believe that this simplification will not affect our conclusions regarding the importance of core excitation.

With this simplification, the kernels can be expanded as

$$K_{\alpha\beta}(R,R') = \sum_{\Lambda\Lambda' S_s \Sigma V} P_{\gamma,\gamma'}^{\Lambda\Lambda' S_s \Sigma V ss_a} F_{\gamma,\gamma'}^{\Lambda\Lambda'\Sigma}(R,R') \tag{14}$$

where γ represents the set of angular momenta $\{l,j,I,L\}$, being l and j the orbital and total angular momentum of the valence particle, L the orbital angular momentum between projectile and target and I the state of the core nucleus b. The unprimed values correspond to the incoming channel and the primed ones to the outgoing channel. $P_{\gamma,\gamma'}^{\Lambda\Lambda' S_s \Sigma V ss_a}$ is a factor that appears due to the recoupling needed to separate the angular momenta which are

spectators in the reaction (the spins of the valence particle, s, and of core a, s_a) from those that actively participate in it (l, L, and I). All the other new angular momenta (Λ, Λ', V, S_s and Σ) appear due to this recoupling. The radial formfactors $F_{\gamma,\gamma'}^{\Lambda\Lambda'\Sigma}(R,R')$ include the actual integration over $\hat{R}$, $\hat{R}'$ and ξ.

The recoupling factors $P_{\gamma,\gamma'}^{\Lambda\Lambda'S_s\Sigma Vss_a}$ have the following expression

$$P_{\gamma,\gamma'}^{\Lambda\Lambda'S_s\Sigma Vss_a} = (-)^{s+s_p+J_p+L+I-J_T+\Lambda'+L'+l'+S_s}$$

$$\times\, \hat{\Lambda}\hat{\Lambda}'\hat{\Sigma}^2\hat{V}^2\hat{S}_s^{\,2}\hat{j}\hat{j}'\hat{J}\hat{J}'\hat{J}_p\hat{J}_t'\begin{Bmatrix} l & s & j \\ s_p & J_p & S_s \end{Bmatrix}$$

$$\times\, \begin{Bmatrix} S_s & l & J_p \\ L & J & \Lambda \end{Bmatrix}\begin{Bmatrix} S_s & \Lambda & J \\ I & J_T & \Sigma \end{Bmatrix}\begin{Bmatrix} l' & L' & \Lambda' \\ s & s_p & S_s \\ j' & J' & V \end{Bmatrix}$$

$$\times\, \begin{Bmatrix} I' & \Lambda' & \Sigma \\ S_s & J_T & V \end{Bmatrix}\begin{Bmatrix} I' & j' & J_t' \\ J' & J_T & V \end{Bmatrix}, \qquad (15)$$

whereas the formfactors $F_{\gamma,\gamma'}^{\Lambda\Lambda'\Sigma}$ have the form

$$F_{\gamma,\gamma'}^{\Lambda\Lambda'\Sigma}(R,R') = \sum (-)^{\Lambda+I'+l'+T+L+\Sigma} q_{\gamma'Q\gamma}^T(R,R')$$

$$\times \begin{pmatrix} l' \\ N' \end{pmatrix}\begin{pmatrix} Q \\ N_C \end{pmatrix}\begin{pmatrix} l \\ N \end{pmatrix}\hat{Q}^2\hat{T}^2\hat{I}'\hat{l}'^2\hat{l}'^2\hat{\Lambda}\hat{\Lambda}'\hat{L}\hat{L}'\hat{F}^2\hat{F}'^2\hat{G}^2\hat{G}'^2\hat{H}^2\hat{R}^2$$

$$\times (a'R)^{N'}(a_c R)^{N_C}(aR)^N (b'R')^{l'-N'}(b_c R')^{Q-N_C}(bR')^{l-N}$$

$$\times \begin{pmatrix} N_C & T & F \\ 0 & 0 & 0 \end{pmatrix}\begin{pmatrix} L' & F & G \\ 0 & 0 & 0 \end{pmatrix}\begin{pmatrix} N & N' & G \\ 0 & 0 & 0 \end{pmatrix}\begin{pmatrix} Q-N_C & T & F' \\ 0 & 0 & 0 \end{pmatrix}$$

$$\times \begin{pmatrix} L & F' & G' \\ 0 & 0 & 0 \end{pmatrix}\begin{pmatrix} l-N & l'-N' & G' \\ 0 & 0 & 0 \end{pmatrix}\begin{Bmatrix} Q & \Lambda & \Lambda' \\ \Sigma & I' & I \end{Bmatrix}$$

$$\times \begin{Bmatrix} F & F' & Q \\ Q-N_C & N_C & T \end{Bmatrix}\begin{Bmatrix} G & F' & H \\ Q & L' & F \end{Bmatrix}\begin{Bmatrix} l' & \Lambda & H \\ Q & L' & \Lambda' \end{Bmatrix}$$

$$\times \begin{Bmatrix} l & l' & R \\ H & L & \Lambda \end{Bmatrix}\begin{Bmatrix} G' & G & R \\ H & L & F' \end{Bmatrix}\begin{Bmatrix} l & R & l' \\ N & G & N' \\ l-N & G' & l'-N' \end{Bmatrix}$$

$$\times \langle I'\|\mathcal{T}_Q^*(\hat{\xi})\|I\rangle, \qquad (16)$$

where the sum is extended over all indices but L, L', Λ, Λ' and Σ, and the limits for the sums are given by the 3-nj symbols, except for N, N' and N_C, which go from 0 to l, l' and Q, respectively. Here $\begin{pmatrix} a \\ b \end{pmatrix} = \sqrt{\dfrac{(2a)!}{(2b)!(2(a-b))!}}$ and the coefficients a, a', a_c, b, b' and b_c are given by Eq. (3). The reduced matrix element $\langle I'\|\mathcal{T}_Q^*\|I\rangle$ is defined with the convention of Brink and Satchler [21].

The quantities $q_{\gamma'Q\gamma}^T(R,R')$ include the radial dependence and are defined as follows:

$$q_{\gamma'Q\gamma}^T(R,R') = \frac{|b|^3}{2}$$

$$\times \int_{-1}^{1} \frac{\varphi_{l',j',I'}'^*(r')}{r'^{l'}}\frac{U_{ab}^Q(r_c)}{r_c^Q}\frac{\varphi_{l,j}(r)}{r^l} P_T(\cos\vartheta)d(\cos\vartheta), \qquad (17)$$

where φ, φ' and U_{ab}^Q are defined in equations (10), (11) and (12), P_T is the Legendre polynomial of degree T, and ϑ is the angle between $\vec{R}$ and $\vec{R}'$. Note that, for the $Q=0$ part of the transition potential, one must calculate also the analogous quantities $q_{\gamma'0\gamma}^T(R,R')$, but using the complete transition potential $V_{av}(r) + U_{ab}^0(r_c) - U_\beta(R')$ instead of U_{ab}^Q.

The formulas of the kernels are more complicated than those obtained for the standard calculations (see, for instance, [20]) due to the coupling of the extra angular momenta Q (multipole of U_{ab}) and I, I' (spin of the core). For the calculations presented in the subsequent sections, the expressions derived above have been implemented in a new DWBA code [22]. The $Q=0$ limit has been tested against the FRESCO code [20].

III. CALCULATIONS

A. The ^{10}Be$(d,p)^{11}$Be reaction

As an application of the formalism presented in the previous section, we consider the stripping reaction of deuterium on ^{10}Be leading to several states of the nucleus ^{11}Be. Since the latter can be modelled as a halo nucleus with a deformed core (^{10}Be), it seems an adequate nucleus to test the importance of these effects. To generate the states of ^{11}Be, we use the particle-rotor model with the parameters given by the set named Be12b in Ref. [23], which were fitted to give the correct separation energies of the ground and first excited states and the position of the low-lying resonances $5/2^+$ and $3/2^+$ at 1.27 MeV and 3.00 MeV above the neutron separation threshold. This model considers only two states of the core, the ground state (0^+) and the first excited state (2^+), with an excitation energy of 3.368 MeV. To represent the resonant states, we use energy bins with a width of 0.8 MeV, obtained with the code FRESCO [20]. For further details on the calculation of multichannel bins we refer to Refs. [20, 24]. The calculated radial parts of the bound states and bin wavefunctions for these states are shown in Fig. 2.

We note that, in this model, the ground, excited and first resonant ($5/2^+$) states have their main component (85%, 79% and 67% of their wavefunctions respectively) with the core in its ground state (0^+). However, the main component (69% of the wavefunction) of the $3/2^+$ resonant state has the ^{10}Be core in its excited state. Therefore, we expect the prompt core excitation effects to be most important for this state of ^{11}Be. As a test of the quality of this particle-rotor model for ^{11}Be, we compare in Table I the spectroscopic factors obtained with the model to those extracted from different experimental data for the 0^+ component of the ground and excited states of ^{11}Be. Due to the difficulty of performing spectroscopy for resonant states, these states are excluded from the comparison. We find that our model tends to
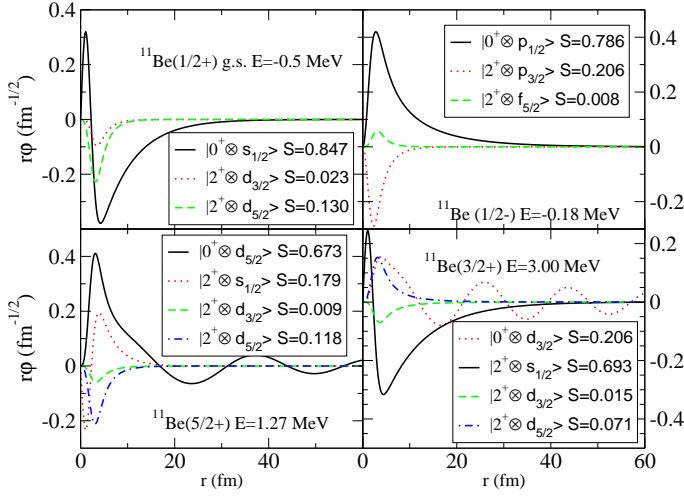
FIG. 2. (Color online) Radial parts of the wave functions for the different states of ^{11}Be considered, obtained by integration of the Schrödinger equation, using energy bins to represent unbound states. The main components (represented by black full lines) correspond to the 0^+ state of the core for the ground state, excited state and resonant $5/2^+$ state, but the main component of the $3/2^+$ resonant state has the core in its excited 2^+ state.
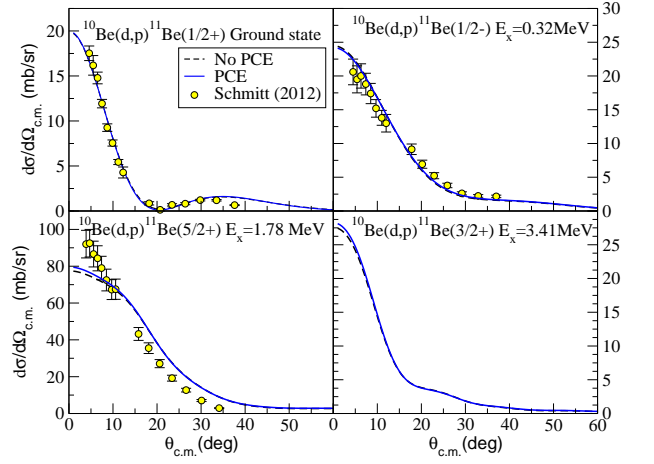

FIG. 3. (Color online) Angular dependence of the cross section of ^{10}Be$(d,p)^{11}$Be to different states of ^{11}Be with incoming energy E_d = 21.4 MeV. Calculations without considering prompt core excitation effects are represented in a black dashed line, while calculations taking them into account are shown with a blue solid line. Experimental data are taken from [25].

overestimate the contribution of the 0^+ component to both ground and excited states as compared to the spectroscopic factors obtained from the analysis of experimental data.

We now calculate the reaction cross section for the transfer reaction ^{10}Be$(d,p)^{11}$Be at an incident energy of 21.4 MeV. At this energy there are experimental data for this reaction for all the considered states of ^{11}Be but the $3/2^+$ resonance [25]. The transition amplitude is evaluated in the ADWA approximation, which is formally identical to the DWBA approximation, but with the deuteron optical potential replaced by an *adiabatic* potential. This potential is not meant to reproduce the elastic scattering, but accounts for the coupling to the breakup channels, which are known to be important for weakly-bound projectiles. In particular, we use the finite-range adiabatic potential of Johnson and Tandy [7], which is constructed based on the $p-^{10}$Be and $n-^{10}$Be potentials. In the calculations presented below, the potentials between $p-^{10}$Be and $n-^{10}$Be are obtained from the global CH89 parametrization [27], omitting spin-orbit terms. This parametrization is also used for the $p-^{11}$Be

potential in the exit channel. For the $p-n$ interaction we have chosen the Gaussian parametrization of Ref. [6] which gives the correct binding energy and rms of the deuteron. We perform two calculations. The first one considers a central $p-^{10}$Be interaction, as done in standard ADWA/DWBA calculations. For the second one, we introduce a quadrupole deformation of this potential with the same quadrupole deformation length parameter, δ_2, (see App. C) as the $n-^{10}$Be potential. Note that this deformation is not considered in the calculation of the adiabatic $d-^{10}$Be potential.

The calculated cross sections are presented in Fig. 3. It can be seen that core excitation effects are negligible for all states. In Table II we give the angle-integrated cross section for both calculations and the relative difference between them for each final state of ^{11}Be. Although this small difference is to be expected for the ground, excited and first resonant states, it is rather surprising for the $3/2^+$ state, since its main component, with an excited 2^+ core, can only be populated in first order by a core excitation mechanism. Remarkable is also the poor agreement with the data for the $5/2^+$ resonance. This discrepancy might be related to the inadequacy of the chosen optical model potentials, to higher order (beyond Born approximation) effects or to the limitations of the reaction formalism employed here to deal with the transfer to unbound states. We note that this is still an open problem [28] but, since our major point of interest is the relative importance of prompt core excitation effects, we have not explored these issues further.

Our results are of the same order of magnitude as those found by Levin [11] for several (d,p) reactions, within a zero-range DWBA model. On the other hand, we find smaller core excitation effects than those reported

TABLE I. Spectroscopic factors for the 0^+ component of ground and excited states of ^{11}Be obtained from particle-rotor potential Be12b [23] and from the analysis of transfer data.

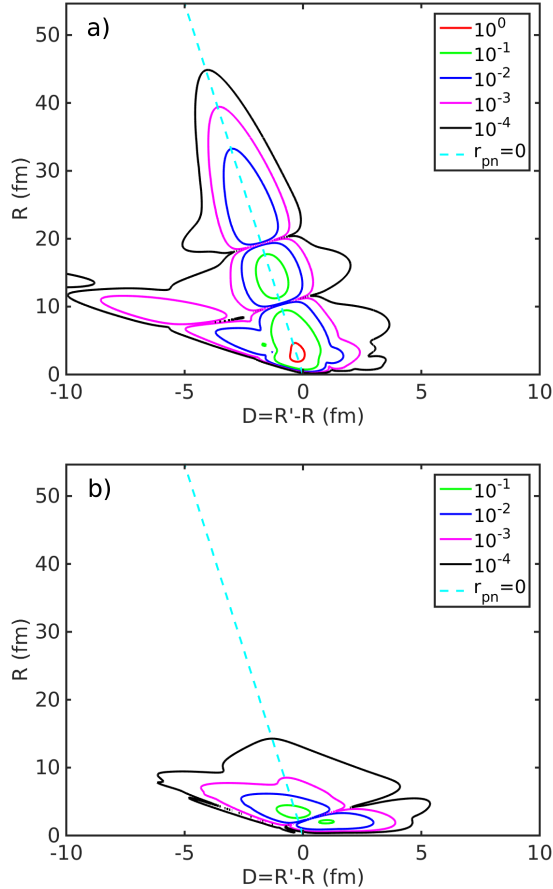| ^{11}Be state	S_{theo} (Be12b)	S_{exp} [25]	S_{exp} [26]
$1/2^+$	0.85	0.74± 0.06	0.73± 0.06
$1/2^-$	0.79	0.65± 0.05	0.63± 0.15

FIG. 4. (Color online) Non-local kernels [see Eqs. (13) and (14)] a) $K_{\alpha\beta}^{(Q=0)}(R, R')$ and b) $K_{\alpha\beta}^{(Q=2)}(R, R')$ for channel $L = 6$, $J = 5$, $L' = 4$, $J' = 7/2$, $J_T = 5$ in the reaction $^{10}\text{Be}(d,p)^{11}\text{Be}$ at $E_d = 21.4$ MeV. Notice that the independent variables are R and $D = R' - R$.

in Ref. [13], where the same data were analysed using the more sophisticated Faddeev formalism. However, as noted in the introduction, those calculations include, in an intricated way, additional core excitation effects, such as the multistep couplings. These effects were in fact found to be significant for the inverse reaction, $^{11}\text{Be}(p,d)^{10}\text{Be}$, according to the CCBA calculations performed in Ref. [29].

We may suggest some possible explanations for the

TABLE II. Cross sections for $^{10}\text{Be}(d,p)^{11}\text{Be}$ at $E_d = 21.4$ MeV, excluding and including prompt core excitation (PCE) effects.

^{11}Be state	σ_{NoPCE} (mb)	σ_{PCE} (mb)	Diff.(%)
$1/2^+$	4.872	4.785	-1.8
$1/2^-$	9.800	10.009	2.1
$5/2^+$	54.10	55.97	3.5
$3/2^+$	7.479	7.717	3.2

smallness of prompt core excitation effects. Firstly, from the expression of the $q_{\gamma'Q\gamma}^T$ functions (17), we see that a certain overlap is required between the wavefunctions of A and B (deuteron and ^{11}Be in our test case) and the multipole of the potential which is considered. Terms with $Q = 0$, which include the potential V_{pn}, are expected to have a greater overlap with deuteron wave functions than terms with higher potential multipoles, which only include $U_{p^{10}\text{Be}}$. This could result in smaller contributions for larger values of Q and, therefore, small effects of core excitation.

Another factor that may affect these results is the large excitation energy of the core (3.368 MeV). This means that, in our particle-rotor model, the effective separation energy of the valence neutron of ^{11}Be is noticeably enhanced when the core is in its excited state, so the exponential decay of its wavefunction as a function of the neutron-core separation will be steeper (let us remark that for all cases considered, the components of ^{11}Be with excited core are effectively bound), as can be seen in Fig.2. Since transfer reactions are peripheral processes, the resulting reduction of the effective radius of ^{11}Be may be relevant to the results obtained.

The combined effects discussed above will tend to make the $Q > 0$ kernels more localized in configuration space as compared to their $Q = 0$ counterparts. This is illustrated in Fig. 4 for the channel $L = 6$, $J = 5$, $L' = 4$, $J' = 7/2$, $J_T = 5$ where the top and bottom panels correspond to the $Q = 0$ and $Q = 2$ contributions. As anticipated, the $Q = 0$ kernels are of longer range, extending to relatively large distances along $r = 0$ (dashed line in the plot). On the contrary, the $Q = 2$ kernels are confined to smaller distances and are comparatively smaller in absolute magnitude, thus explaining the reduced effect on the transfer cross sections.

Since one of the reasons for this smallness of the core-excitation effects in the $^{10}\text{Be}(d,p)^{11}\text{Be}$ reaction is the relatively high excitation energy of the core, one may speculate that these effects will be enhanced in other systems, for which this is excitation energy is smaller. This is quantitatively tested in the next subsection.

B. Calculation with reduced core excitation energy

In order to study the influence of the excitation energy of the core on prompt core excitation effects, we have artificially reduced the excitation energy of ^{10}Be to 0.10 MeV so as to obtain a bound $3/2^+$ state at -0.16 MeV. The main component of this shifted state (88% of the wavefunction) has its core in its excited 2^+ state and it is bound, so the problems of transfer to the continuum should be avoided. The radial parts of the wavefunction corresponding to this state are shown in Fig. 5. We now perform calculations of the transfer reaction $^{10}\text{Be}(d,p)^{11}\text{Be}$ to this artificial state for different energies of the incoming projectile: 21.4, 30, 40, 60 and 100 MeV. The angle-integrated transfer cross sections
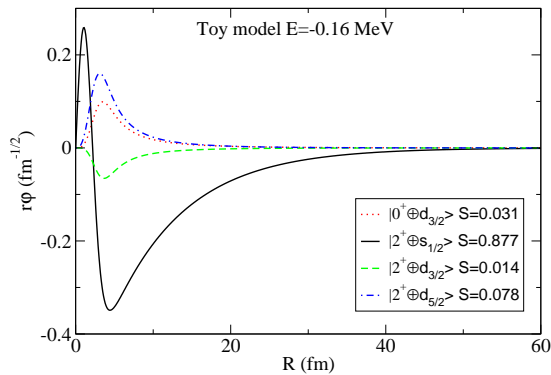
FIG. 5. (Color online) Radial parts of the wave function for the artificially bound state of ^{11}Be built with an excitation energy for the core of ^{10}Be of 0.1 MeV. The spectroscopic factors corresponding to each component are shown in the legend.
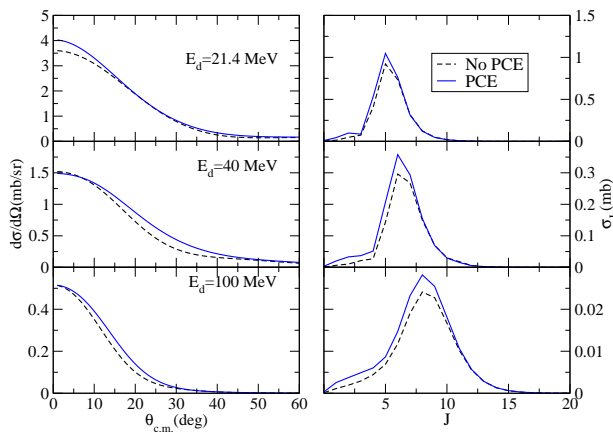

FIG. 6. (Color online) Angular (left) and total angular momentum (right) dependence of ^{10}Be(d,p)^{11}Be reaction cross section to the artificially bound $3/2^+$ state of ^{11}Be defined in the text for energies of the incident deuteron of 21.4, 40 and 100 MeV.

are listed in Table III and the angular dependence and total angular momentum dependence of the transfer cross section are shown in Fig. 6.

We observe that the effects become much more important when transferring a neutron to this artificial state with reduced core energy. From Fig. 6 and Table III

TABLE III. Cross sections for ^{10}Be(d,p)^{11}Be, to the artificially bound $3/2^+$ state described in the text, excluding and including prompt core excitation (PCE) effects.

E_d (MeV)	σ_{NoPCE} (mb)	σ_{PCE} (mb)	Diff.(%)
21.4	2.72	3.09	13.5
30	1.68	2.01	19.5
40	1.05	1.28	22.0
60	0.458	0.564	23.0
100	0.133	0.158	18.6

we see that the total transfer reaction cross section is reduced with increasing incoming energy. It is noticeable the weak dependence of the relative importance of prompt core excitation effects with projectile energy, which seems to indicate that, in a range of $10-50$ MeV per nucleon, these effects will contribute to the same proportion of the cross section. Therefore, their study at smaller energies, favoured due to the larger cross sections, should be useful when predicting their relevance at higher energies.

From this study we can conclude that prompt core excitation effects will be important when transferring particles between nuclei with cores with small excitation energies, and that their contributions are expected to vary slowly with energy. For example, very neutron-rich Ne, Na and Mg isotopes around the so-called *island of inversion* are characterized by small 2^+ excitation energies and hence are expected to be good candidates to exhibit non-negligible prompt core excitation effects. An example of this is considered in the next subsection.

C. ^{30}Ne(d,p)^{31}Ne

As a final example, we consider the reaction ^{30}Ne(d,p)^{31}Ne at an incident energy of 30 MeV. The structure of the ^{31}Ne nucleus is not completely known, but most studies suggest a halo-like structure with a weakly bound neutron with a mixed $p_{3/2}/f_{7/2}$ configuration. A combined analysis of 1n-removal experiment of this nucleus on C and Pb targets performed at RIKEN at 230 MeV/nucleon [30] gives $S_n = 0.15^{+0.16}_{-0.10}$ MeV, and a spin-parity $3/2^-$. The first excited state of the core (2^+) is located at $E_x \approx 800$ keV, so core excitation effects are expected to be significantly larger than in the ^{11}Be case.

The ^{31}Ne nucleus has been studied in the particle-rotor model by Urata *et al.* [31, 32]. However, the validity of this model for this nucleus is still unclear so, for the transfer calculations presented in this work, we will rely on a phenomenological model of ^{31}Ne with spectroscopic factors quoted in Ref. [30] (model SM(ii)), obtained from shell-model calculations using the modified monopole $sd - pf$ cross-shell SDPF-M interaction. The spectroscopic factors are 0.21, 0.33 and 0.80 for the $[0_1^+ \otimes 2p_{3/2}]$, $[2_1^+ \otimes 2p_{3/2}]$ and $[2_1^+ \otimes 1f_{7/2}]$ configurations, respectively. In combination with eikonal calculations, these spectroscopic factors give knockout cross sections in good agreement with the experimental data of Ref. [30]. The radial parts of the bound state wavefunction and their relative signs are obtained from a particle-rotor calculation, similar to that of Refs. [31, 32], but the normalization of each component was taken from the spectroscopic factors quoted above. The deformation parameter of the core-target potential was taken as $\beta_2 = 0.2$ [32]. As in our previous calculations, the potentials have been calculated with the CH89 global parametrization [27], the finite-range potential of Johnson and Tandy [7] and the Gaussian deuteron potential of Ref. [6].
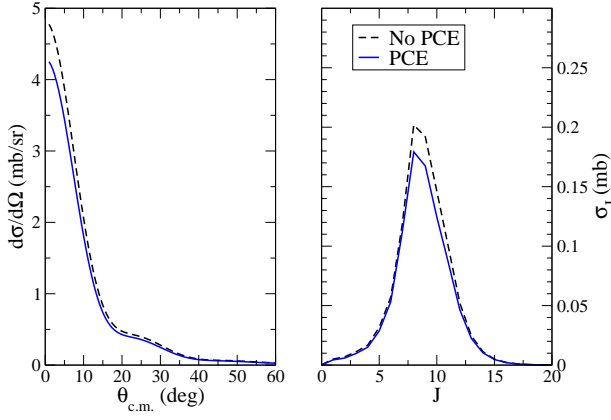
FIG. 7. (Color online) a) Angular distribution and b) angular momentum dependence for the ^{30}Ne$(d,p)^{31}$Ne reaction at 30 MeV, with the inclusion and omission of prompt core excitation effects. The model used for ^{31}Ne is described in the text.

In Fig. 7 we plot the calculated angular distributions, with and without core excitation. The difference between both calculations is about $\sim 11\%$, still a modest value, but significantly larger than in the ^{10}Be(d,p) case, as anticipated.

From these calculations it can be concluded that the effects of prompt core excitation are in general small but not negligible, with an influence on the cross section of the order of $\sim$2–10%. Since these effects become more important when the excitation energy of the core is reduced, they may play a greater role in transfer reactions with more massive nuclei. Also, in reactions with less halo-like nuclei, where the influence of the core might be more important, these effects may become more relevant and should be taken into account when obtaining spectroscopic factors from transfer cross sections.

IV. SUMMARY AND CONCLUSIONS

We have developed a formalism to include prompt core excitation effects in transfer reactions within the DWBA approximation. The formalism accounts for the transition between different core states of the initial and final nuclei due to the presence of non-central terms in the core-core interaction appearing in the transition operator. For the cases considered in this work, we have adopted a collective model of the core-core interaction, which has been described in terms of a deformed potential. We have shown that the developed formalism reduces to the standard DWBA expression when a central potential is used for the core-core interaction (see App. B).

We have studied the influence of these effects on the ^{10}Be$(d,p)^{11}$Be and ^{30}Ne$(d,p)^{31}$Ne transfer reactions. In the former case, the effect of prompt core excitation is very small, with a contribution of $\sim 2-4\%$ to the trans-

fer cross section. This is attributed in part to the relatively high excitation energy of the core, which leads to a large effective separation energy of the neutron in the configurations with an excited core, and hence to more localized non-local kernels. This reduces the effective radius of ^{11}Be with an excited core, and its contribution to a peripheral reaction such as transfer.

In the ^{30}Ne$(d,p)^{31}$Ne case, for which the excitation energy of the core is much smaller ($\sim$ 800 keV) the core excitation mechanism enhances the transfer cross section by 11%, and therefore the effect is no longer negligible.

Although the calculations presented in this work are based on the DWBA approximation, the formalism could be extended to more sophisticated formalisms, such as CCBA. In the latter case, additional core-excitation effects would be present in the form of multistep couplings.

Appendix A: Construction of the kernels

In this appendix, we give an overview on the steps taken in order to obtain the kernel from equation (14). The complete derivation is rather lengthy so we outline here only the main steps. As mentioned in Sec. II, the term $P_{\gamma,\gamma'}^{\Lambda\Lambda' S_s \Sigma V s s_a}$ results from the recouplings

$$|[[L, \{(l,s)j, s_a\}J_p] J, J_t] J_T M_T\rangle$$
$$\rightarrow |[[(L,l)\Lambda, I] \Sigma, (s, s_a)S_s] J_T M_T\rangle \quad (A1)$$
$$|[[L', J'_p] J', \{(l',s)j', I'\}J'_t] J_T M_T\rangle$$
$$\rightarrow |[[(L',l')\Lambda', I'] \Sigma, (s, s_a)S_s] J_T M_T\rangle \quad (A2)$$

From the definition of the 6j symbol [21] and the one of the 12j symbol given by Jahn and Hope [33] as well as its expansion in 6j and 9j symbols, the expression of $P_{\gamma,\gamma'}^{\Lambda\Lambda' S_s \Sigma V s s_a}$ can be obtained, bearing in mind that s and s_a are not modified in the reaction and that $J_t = I$ and $J'_p = s_a$.

As for $F_{\gamma,\gamma'}^{\Lambda\Lambda'\Sigma}$, it involves the integration in the angular coordinates of $\vec{R}$ and $\vec{R}'$. Therefore, all angular dependences must be expressed in terms of these two coordinates. For this, we make use of the solid harmonics expansion [34]:

$$r^Q C_{Qq}(\hat{r}) = \sum_{Nn} \binom{Q}{N} (aR)^N (bR')^{Q-N} \hat{Q}(-1)^{Q+q}$$
$$\times \begin{pmatrix} Q-N & N & Q \\ q-n & n & -q \end{pmatrix} C_{Nn}(\hat{R}) C_{Q-N,q-n}(\hat{R}'),$$
$$(A3)$$

with $\vec{r} = a\vec{R} + b\vec{R}'$ and where the definitions of Sec. II apply. This formula is applied to the spherical harmonics that appear from $\varphi'_{\gamma'}(\vec{r'})$, $\varphi_\gamma(\vec{r})$ and $C_{Qq}(\vec{r_c})$ from expansion (12).

In order to extract the dependence on $\hat{R}$ and $\hat{R}'$ from the moduli of $\vec{r}$, $\vec{r'}$ and $\vec{r_c}$ we perform an expansion on

multipoles of the product of the radial part of the wave-functions of A and B and the multipole of the potential:

$$
\frac{\varphi *'_{\gamma'}(r')}{r'^{l'}}\frac{U_{ab}^Q(r_{cc})}{r_{cc}^Q}\frac{\varphi_\gamma(r)}{r^l} = \sum_{Tt}\hat{T}^2(-1)^t
$$
$$
\times q_{\gamma'Q\gamma}^T(R,R')C_{Tt}(\hat{R})C_{T-t}(\hat{R}'). \tag{A4}
$$

From this expansion we obtain the radial $q_{\gamma'Q\gamma}^T$ functions from (17), which only depend on the moduli R and R', and two extra spherical harmonics, one in $\hat{R}$ and another in $\hat{R}'$. Considering also the angular part of the incoming and outgoing distorted waves, we have a total of 5 spherical harmonics dependent on $\hat{R}$ and $\hat{R}'$. In order to perform the integration we reduce their number to three, using the property:

$$
C_{Aa}(\hat{R})C_{Bb}(\hat{R}) = \sum_{Cc}\hat{C}^2(-1)^c C_{Cc}(\hat{R})
$$
$$
\times \begin{pmatrix} A & B & C \\ 0 & 0 & 0 \end{pmatrix}\begin{pmatrix} A & B & C \\ a & b & -c \end{pmatrix}, \tag{A5}
$$

and finally integrate analitically using

$$
\int d\hat{R}\, C_{Aa}(\hat{R})C_{Bb}(\hat{R})C_{Cc}(\hat{R}) = 4\pi \begin{pmatrix} A & B & C \\ 0 & 0 & 0 \end{pmatrix}\begin{pmatrix} A & B & C \\ a & b & c \end{pmatrix}. \tag{A6}
$$

The integration on ξ is made symbolically, through the reduced matrix element $\langle I'\|\mathcal{T}_Q^*\|I\rangle$, obtained with the Wigner-Eckart theorem and Brink and Satchler's convention [21]:

$$
\langle I'i'|\mathcal{T}_{Qq}^*(\hat{\xi})|Ii\rangle = (-1)^{I'-i'}\hat{I}'\begin{pmatrix} I' & Q & I \\ -i' & q & i \end{pmatrix}\langle I'\|\mathcal{T}_Q^*(\hat{\xi})\|I\rangle \tag{A7}
$$

After performing the integrals, the resulting 3j symbols (in our calculations 20 of them appear) can be added symbolically, to give a more compact result. For this, the graphical method of Yutsis, Levinson and Vanagas [21, 35, 36] has been very useful. This simplification is the last step to obtain the formula (16) for the radial form factors $F_{\gamma,\gamma'}^{\Lambda\Lambda'\Sigma}$.

Appendix B: $Q = 0$ limit

If one considers a central U_{ab} potential, then $Q = 0$, and many simplifications apply to the expression (14). The reduced matrix element $\langle I'\|\mathcal{T}_Q^*\|I\rangle$ becomes $\delta_{I',I}$, and therefore no prompt core excitation is allowed. $Q = 0$ implies $N_C = 0$ and many 3j and 6j symbols can be reduced to Kronecker deltas, which allow summation over indices H, F, and F', and obtaining $\Lambda = \Lambda'$. After these simplifications the expression of $F_{\gamma,\gamma'}^{\Lambda\Lambda'\Sigma}$ reduces to:

$$
F_{\gamma,\gamma'}^\Lambda = \sum(-)^{\Lambda+L'+T+L}q_{\gamma'0\gamma}^T(R,R')\begin{pmatrix} l' \\ N' \end{pmatrix}\begin{pmatrix} l \\ N \end{pmatrix}
$$
$$
\times \hat{T}^2\hat{l}^2\hat{l}'^2\hat{L}\hat{L}'\hat{G}\hat{G}'^2\hat{R}^2(a'R)^{N'}(aR)^N
$$
$$
\times (b'R')^{l'-N'}(bR')^{l-N}\begin{pmatrix} L' & T & G \\ 0 & 0 & 0 \end{pmatrix}
$$
$$
\times \begin{pmatrix} N & N' & G \\ 0 & 0 & 0 \end{pmatrix}\begin{pmatrix} L & T & G' \\ 0 & 0 & 0 \end{pmatrix}\begin{pmatrix} l-N & l'-N' & G' \\ 0 & 0 & 0 \end{pmatrix}
$$
$$
\times \begin{Bmatrix} l & l' & R \\ L' & L & \Lambda \end{Bmatrix}\begin{Bmatrix} G' & G & R \\ L' & L & T \end{Bmatrix}\begin{Bmatrix} l & R & l' \\ N & G & N' \\ l-N & G' & l'-N' \end{Bmatrix}. \tag{B1}
$$

Since $F_{\gamma,\gamma'}^\Lambda$ no longer depends on Σ it is possible to sum over it, which simplifies the expression of $P_{\gamma,\gamma'}^{\Lambda\Lambda'S_s\Sigma Vss_a}$ to:

$$
P_{\gamma,\gamma'}^{\Lambda S_s ss_a} = (-)^{s+s_p+J_p+L+I-J_T+\Lambda+L'+l'+S_s}
$$
$$
\times \hat{\Lambda}^2\hat{S}_s{}^2\hat{j}\hat{j}'\hat{J}\hat{J}'\hat{J}_p\hat{J}_t'\begin{Bmatrix} l & s & j \\ s_p & J_p & S_s \end{Bmatrix}\begin{Bmatrix} S_s & l & J_p \\ L & J & \Lambda \end{Bmatrix}
$$
$$
\times \begin{Bmatrix} l' & L' & \Lambda \\ s & s_p & S_s \\ j' & J' & J \end{Bmatrix}\begin{Bmatrix} I' & j' & J_t' \\ J' & J_T & J \end{Bmatrix}, \tag{B2}
$$

which can be shown to be equivalent to the standard expression given, for instance, in Ref. [20].

Appendix C: Particle-rotor model

For our calculations, we have adopted a particle-rotor model for the ^{11}Be and ^{31}Ne nuclei. In this model, the core nucleus is assumed to have a permanent quadrupole deformation which, for simplicity, is taken to be axially symmetric. Thus, the deformation is characterized by a single collective parameter, β_2. In the body-fixed frame, the radius of the surface is parametrized as $R(\xi) = R_0(1 + \beta Y_{20}(\xi))$, with R_0 an average radius. Starting from a central potential, $V_{vc}^{(0)}(r)$, the valence–core interaction is obtained by deforming this interaction as

$$
V_{vc}(\vec{r},\xi) = V_{vc}^{(0)}(r - \delta_2 Y_{20}(\xi)), \tag{C1}
$$

with $\delta_2 = \beta_2 R_0$, usually referred to as deformation length. This expression is transformed to the space-fixed reference frame, and expanded in spherical harmonics (see e.g. Ref. [37])

$$
V_{vc}(r,\theta,\phi) = \sum_{\lambda\mu}\hat{\lambda}\,\mathcal{V}_{vc}^\lambda(r)\mathcal{D}_{\mu 0}^\lambda(\alpha,\beta,\gamma)C_{\lambda\mu}(\hat{r}), \tag{C2}
$$

where $\mathcal{D}_{\mu 0}^\lambda$ is a rotation matrix, $\{\alpha,\beta,\gamma\}$ are the Euler angles defining the transformation from the body-fixed

frame to the space-fixed frame and $\mathcal{V}_{vc}^{\lambda}(r)$ the radial form factors

$$\mathcal{V}_{vc}^{\lambda}(r) = \frac{\hat{\lambda}}{2}\int_{-1}^{1}V_{vc}(\vec{r},\xi)P_{\lambda}(\cos\theta)d(\cos\theta), \quad \text{(C3)}$$

with θ is the angle between $\vec{r}$ and ξ and all other relevant definitions can be found in Sec. II.

Analogously, the core-core interaction, U_{ab} is generated also starting from a spherical optical potential, which is then deformed with the same deformation length δ_2, and expanded in multipoles as

$$U_{ab}(r_c,\theta',\phi') = \sum_{Qq}\hat{Q}\,U_{ab}^{Q}(r_c)\mathcal{D}_{q0}^{Q}(\alpha',\beta',\gamma')C_{Qq}(\hat{r}_c),\,\text{(C4)}$$

giving rise to the radial form factors

$$U_{ab}^{Q}(r_c) = \frac{\hat{Q}}{2}\int_{-1}^{1}U_{ab}(\vec{r}_c,\xi)P_{Q}(\cos\theta)d(\cos\theta), \quad \text{(C5)}$$

where θ is now the angle between $\vec{r}_c$ and ξ.

Comparing (C4) with the general expansion (12) we see that, in the rotational model, $\mathcal{T}_{Qq}^{*}(\xi) \equiv \mathcal{D}_{q0}^{Q}(\alpha',\beta',\gamma')$. The reduced matrix elements entering the expression of the non-local kernels [Eq. (16)] are just the reduced matrix elements of the rotation matrix between the core eigenstates which, in the case of a rigid rotor with axial symmetry, are given by (see e.g. Ref. [38])

$$\langle\xi|I\rangle = \frac{\hat{I}}{\sqrt{8\pi^2}}\mathcal{D}_{K0}^{I}(\xi), \quad \text{(C6)}$$

with K is the projection of $\vec{I}$ along the space-fixed frame. The required reduced matrix elements result

$$\langle I'\|\mathcal{T}_Q^*\|I\rangle = (-1)^{I'}\hat{I}\begin{pmatrix} I' & Q & I \\ 0 & 0 & 0 \end{pmatrix} \quad \text{(C7)}$$

where the convention of Brink and Satchler for reduced matrix elements has been assumed.

ACKNOWLEDGMENTS

[1] G. R. Satchler, *Direct Nuclear Reactions* (Clarendon Press, Oxford, 1983)
[2] G. H. Rawitscher, Phys. Rev. C **11**, 1152 (1975)
[3] Y. Iseri, M. Yahiro, and M. Nakano, Progress of Theoretical Physics **69**, 1038 (1983)
[4] H. Amakawa and N. Austern, Phys. Rev. C **27**, 922 (1983)
[5] M. Kawai, Progress of Theoretical Physics Supplement **89**, 11 (1986)
[6] N. Austern, Y. Iseri, M. Kamimura, M. Kawai, G. Rawitscher, and M. Yahiro, Phys. Rep. **154**, 125 (1987)
[7] R. C. Johnson and P. C. Tandy, Nucl. Phys. A **235**, 56 (1974)
[8] L. D. Faddeev, Zh. Eksp. Theor. Fiz. **39**, 1459 (1960), [Sov. Phys. JETP **12**, 1014 (1961)]
[9] E. O. Alt, P. Grassberger, and W. Sandhas, Nucl. Phys. B **2**, 167 (1967)
[10] J. G. Camacho and A. M. Moro, in *The Euroschool on Exotic Beams, Vol. IV* (Springer, 2014) pp. 39–66
[11] F. Levin, Phys. Rev. **147**, 715 (1966)
[12] B. Kozlowsky and A. De-Shalit, Nucl. Phys. **77**, 215 (1966)
[13] A. Deltuva, Phys. Rev. C **88**, 011601 (2013)
[14] R. Crespo, A. Deltuva, and A. M. Moro, Phys. Rev. C **83**, 044622 (2011)
[15] A. M. Moro and R. Crespo, Phys. Rev. C **85**, 054613 (2012)
[16] A. M. Moro and J. A. Lay, Phys. Rev. Lett. **109**, 232502 (2012)
[17] R. Johnson, Journal of Physics G: Nuclear and Particle Physics **41**, 094005 (2014)
[18] N. K. Glendenning, *Direct Nuclear Reactions* (World Scientific Publishing, 2004)
[19] R. de Diego, J. M. Arias, J. A. Lay, and A. M. Moro, Phys. Rev. C **89**, 064609 (2014)
[20] I. J. Thompson, Computer Physics Reports **7**, 167 (1988)
[21] D. M. Brink and G. R. Satchler, *Angular Momentum* (Clarendon Press, Oxford, 1968)
[22] M. Gomez-Ramos and A. M. Moro, Unpublished (2014)
[23] F. M. Nunes, J. A. Christley, I. J. Thompson, R. C. Johnson, and V. D. Efros, Nucl. Phys **A609**, 43 (1996)
[24] N. C. Summers, F. M. Nunes, and I. J. Thompson, Phys. Rev. C **74**, 014606 (2006)
[25] K. T. Schmitt *et al.*, Phys. Rev. Lett. **108**, 192701 (2012)
[26] D. L. Auton, Nucl. Phys. **A157**, 305 (1970)
[27] R. Varner, W. Thompson, T. McAbee, E. Ludwig, and T. Clegg, Physics Reports **201**, 57 (1991)
[28] J. E. Escher, I. J. Thompson, G. Arbanas, C. Elster, V. Eremenko, L. Hlophe, and F. M. Nunes (TORUS Collaboration), Phys. Rev. C **89**, 054605 (2014)
[29] J. Winfield *et al.*, Nuclear Physics A **683**, 48 (2001)
[30] T. Nakamura *et al.*, Phys.Rev.Lett. **112**, 142501 (2014)

[31] Y. Urata, K. Hagino, and H. Sagawa, Phys.Rev. C **83**, 041303 (2011)

[32] Y. Urata, K. Hagino, and H. Sagawa, Phys.Rev. C **86**, 044613 (2012)

[33] H. A. Jahn and J. Hope, Phys. Rev. **93**, 318 (1954)

[34] M. Moshinsky, Nuclear Physics **13**, 104 (1959)

[35] A. P. Yutsis, J. B. Levinson, and V. V. Vanagas, *Mathematical Apparatus of the Theory of Angular Momentum* (Israel Program for Scientific Translation, 1962)

[36] D. Varshalovich, A. N. Moskalev, and V. K. Khersonskii, *Quantum Theory of Angular Momentum* (World Scientific, 1988)

[37] T. Tamura, Rev. Mod. Phys. **37**, 679 (1965)

[38] P. Ring and P. Schuck, *The Nuclear Many-Body Problem* (Springer Editorial, 2000)